ELSEVIER

Chemical Engineering Journal 136 (2008) 41–49

Chemical Engineering Journal

www.elsevier.com/locate/cej

Oxidative steam reforming of ethanol over Ni/CeO_2-ZrO_2 catalyst

Prakash Biswas, Deepak Kunzru *

Department of Chemical Engineering, Indian Institute of Technology Kanpur, Kanpur 208016, UP, India

Received 18 September 2006; received in revised form 15 February 2007; accepted 20 March 2007

Abstract

Catalytic steam reforming of ethanol for hydrogen production in presence and absence of oxygen has been studied over Ni-CeO_2-ZrO_2 catalyst. The effect of oxygen addition and space time on conversion and product selectivities has been investigated in a down-flow tubular fixed bed reactor at atmospheric pressure with an ethanol/water molar ratio of 1:8, over a temperature range of 400–650 °C. The O_2/EtOH molar ratio was varied from 0.5 to 1.5. In the presence of oxygen, the catalytic activity was significantly higher and the effect was more at lower temperature (<450 °C). Hydrogen yields and selectivities as well as the coke deposition were significantly affected by addition of oxygen. At a temperature ≤500 °C, hydrogen yield was highest at an O_2/EtOH molar ratio of 0.5, whereas at higher temperatures, higher hydrogen yields were obtained in absence of oxygen. Higher oxygen content in the feed (O_2/EtOH ≥ 0.5) reduced the hydrogen yield.

Keywords: Nickel; Oxidative steam reforming; Ethanol; Hydrogen production

1. Introduction

In recent year, considerable effort has been expended in developing fuel cells. Fuel cells not only eliminate toxic emissions but also have a higher efficiency than internal combustion engines for converting chemical energy of the fuel to electrical energy. The choice of fuel for the fuel cell technology could become a very important aspect in establishing environmental impact and the cost of produced electricity. Progress and recent trends on the production and utilization of bio-fuel have been discussed [1,2]. Hydrogen production from renewable sources such as biomass, is gaining attention as a CO_2 neutral energy supply [3]. Alcohols are potentially attractive feedstocks for producing hydrogen for use in fuel cells [4] and methanol steam reforming has been extensively studied [5–9]. However, the main drawback of methanol is its high toxicity and that it is produced from non-renewable sources. On the other hand, ethanol can be produced by fermentation of renewable resources such as biomass and is also less toxic than methanol. Moreover, it is easy to transport, biodegradable and can be easily reformed in the presence of water to generate a hydrogen-rich mixture that is free from sulfur [10–12].

Hydrogen can be obtained directly from ethanol by steam reforming (SR), partial oxidation (PO) or oxidative steam reforming (OSR). SR generates a high H_2/CO ratio but has the disadvantage of high endothermicity and catalyst deactivation due to coke deposition. On the other hand, PO is exothermic but it generates a lower H_2/CO ratio than SR. OSR is a combination of PO and SR and can produce suitable H_2/CO ratio without external energy consumption. OSR seems to be a reasonably good alternative whose salient features are reduced rate of carbon deposition and more favorable thermal equilibrium that can be varied as a function of the oxygen feed [13].

Ethanol steam reforming has been investigated on several catalyst systems and has been recently reviewed [14–19]. Most of the catalysts are Ni-based, either undoped or doped with other metals such as Cu, Cr, Zn or K. Fierro et al. [20] tested different metals for OSR and the order of activity for hydrogen production was Ni–Zn > Ni–Fe > Ni–Cr > Ni–Cu. Production of hydrogen by SR was strongly influenced by the addition of small amount of oxygen [21,22]. Velu et al. [23] tested the OSR reaction of bio-ethanol using a series of CuNiZnAl multicomponent mixed metal catalysts with various Cu/Ni ratios. They observed that Cu rich catalyst favored ethanol to acetaldehyde

* Corresponding author. Tel.: +91 512 2597193; fax: +91 512 2590104.
E-mail address: dkunzru@iitk.ac.in (D. Kunzru).

1385-8947/$ – see front matter © 2007 Elsevier B.V. All rights reserved.
doi:10.1016/j.cej.2007.03.057

dehydrogenation reaction whereas addition of Ni promoted the C–C bond rupture. Frusteri et al. [24] studied steam and autothermal reforming of bio-ethanol over Ni/MgO and Ni/CeO_2 catalysts. The performance of both the catalysts was enhanced at an optimum O_2/C ratio mainly due to the reduction in coke formation. Earlier studies [25,26] have shown that addition of ZrO_2 into CeO_2, improves the redox property, oxygen storage capacity and thermal stability, resulting in better performance in CO oxidation and methane combustion. Pengpanich et al. [27] reported that Ni/Ce-ZrO_2 showed a good resistance to coke formation in ethane partial oxidation reaction.

In our previous study [28], we have investigated the SR of ethanol (without added oxygen) on nickel supported on $Ce_{1-x}Zr_xO_2$ ($x = 0$, 0.26, 0.59, 0.84 and 1) catalysts. The most promising catalyst was 30% Ni/$Ce_{0.74}Zr_{0.26}O_2$. In this study, the oxidative reforming of ethanol over 30%Ni/$Ce_{0.74}Zr_{0.26}O_2$ catalyst was investigated focusing attention on reaction parameters such as temperature, space time and oxygen concentration on catalyst activity, product selectivity and hydrogen yields.

2. Experimental

2.1. Catalyst preparation

The CeO_2-ZrO_2 mixed oxide support was prepared by co-precipitation with ammonia using aqueous solution of cerium nitrate and zirconium oxychloride. Aqueous ammonia solution was added dropwise to the aqueous solution containing the Ce and Zr salt at the appropriate composition with constant stirring until pH was 9–10. After precipitation, the obtained hydroxide was filtered, washed thoroughly with deionized water, and then dried at 120 °C for 12 h. The obtained solid was calcined in air at 750 °C for 5 h. The resulting solid oxide was crushed and sieved to a size 50–70 mesh before metal impregnation.

30 wt.%Ni loading was carried out by incipient wetness impregnation method. After impregnation, the catalyst was dried at 120 °C for 12 h and then calcined at 500 °C for 5 h.

2.2. Catalyst characterization

The specific surface area of catalysts was determined by the dynamic pulsing technique on a Micromeritics 2705 instrument, employing nitrogen physio-sorption at liquid nitrogen temperature. The XRD spectra were obtained with a Siemmens diffractometer (Model D500) using Cu Kα radiation, Ni filter and 40 kV, at a two theta interval of 20–100° with a sweep of 3°/min and a time constant of 3 s. The H_2-TPR analysis was obtained on a Micromeritics Pulse Chemisorb 2705 unit, using 25 mg of catalyst and a temperature ramp from 35 to 1000 °C at 10 °C/min. A flow rate of 40 cm^3 /min of 5% H_2 in Ar was used for the reduction. Hydrogen pulse chemisorption was also carried out on Micromeritics 2705 at 50 °C using pure H_2. The pulse was given after 3–5 min interval until the areas of successive hydrogen peaks were identical.

The surface morphology of fresh and used catalysts was analyzed by transmission electron microscopy (TEM) on a JEM-2000 FX-II unit. The samples for TEM analysis were prepared by ultrasonic dispersion of the catalysts in absolute ethanol. One drop of this solution was put on the carbon-coated copper grid (400 mesh) and the grid then was dried under ambient conditions.

The amount of carbon deposited on the catalyst after SR and OSR reaction was determined by CHNS elemental analysis using an Elemental Analyzer (Model: CE440, Leeman Labs Inc., USA). Approximately 5 mg of used catalyst was taken and treated in the presence of oxygen at 960 °C. The CO_2 produced by the oxidation of the sample was analyzed by a thermal conductivity detector.

2.3. Catalyst testing

The details of the experimental set-up and procedure have been reported earlier [28]. The experiments were performed at atmospheric pressure in a continuous fixed bed down-flow quartz tubular reactor. The catalyst (size 50–80 mesh) was diluted with quartz particles of the same size and placed on a quartz wool bed inside the reactor. Prior to a run, the catalyst was reduced *in situ* at 700 °C for 1 h under a hydrogen flow. Nitrogen, which served as an inert, was mixed with the vaporized feed, and the mixture was then fed to the reactor. The flow rate of nitrogen was controlled by a mass flow controller. The water/ethanol molar ratio was kept at 8:1; the O_2/EtOH molar ratio was varied from 0.5 to1.5 and the reaction temperature from 400 to 650 °C.

Initially, the activity declined at a relatively faster rate, but after 4 h of reaction, the rate of deactivation was very low. Therefore, all the data were collected after 4 h of reaction and the run time for each run was 1 h. The carbon balance was 100 ± 5%.

The selectivity of carbon containing products has been defined as:

$$S_X(\%) = \frac{\text{moles of carbon in product } X}{\text{total moles of hydrogen in products}} \times 100$$

and the selectivity to hydrogen as:

$$S_{H_2}(\%) = \frac{\text{moles of } H_2 \text{ produced}}{\text{total moles of hydrogen in products}} \times 100$$

3. Results and discussion

The surface area of the catalyst was 19.5 m^2/g, the metal area 0.30 m^2/g and nickel dispersion was 0.3%. This is comparable to the values reported by Laosiripojana and Assabumrungrat [29] for ceria-zirconia supported nickel catalysts. The average crystallite size of the support ($Ce_{0.74}Zr_{0.26}O_2$) was estimated from X-ray line width of the peak corresponding to (1 1 1) and (2 2 0) crystal planes and for NiO from (1 1 1), (2 2 0) and (3 1 1) crystal planes, respectively, using Scherrer equation [30]. The dimension of CeO_2-ZrO_2 crystallites was 12.5 nm, whereas the NiO crystallite was 17.3 nm.

The degree of reduction of nickel was calculated from the TPR results by assuming that the degree of reduction of support in Ni/Ce-ZrO_2 was the same as for pure Ce-ZrO_2 support. The results showed that 78.1% of NiO in the catalyst was reduced.

3.1. Non-catalytic oxidative steam reforming of ethanol

To determine the extent of homogeneous reactions in the presence of oxygen, experiments were carried out with only quartz powder (250 mg) placed in the reactor. The molar ratios of H_2O/EtOH and O_2/EtOH were kept fixed at 8 and 0.5, respectively, and the flow of ethanol was 4.1×10^{-4} mol/min. The effect of temperature on conversion of ethanol and product selectivity in absence of catalyst is shown in Fig. 1. Ethanol conversion was significant above 500 °C, reaching 99% at 650 °C, and the oxygen conversion was complete. In addition to H_2, CO, CH_4 and CO_2, others products such as C_2H_4, CH_3CHO and CH_3COCH_3 were also observed. As shown in Fig. 1, selectivity to H_2, CO, CH_4 and C_2H_4 increased with temperature. The maximum selectivity to hydrogen was 35.4% which is significantly lower than the maximum possible selectivity. Selectivity to CO_2 showed a minima at 500 °C, whereas the selectivity to CH_3CHO was relatively high at lower temperature and decreased sharply at higher temperature, but was still 8.4% at 650 °C. Beyond 500 °C, the selectivity to CH_3COCH_3 was nearly zero. Selectivity to C_2H_4 varied from 5.3 to 23%; this is rather important, because ethylene acts as a very strong promoter of carbon formation. The product distribution shows that at low temperatures dehydrogenation of ethanol to CH_3CHO was predominant. The low value of hydrogen selectivities indicate that a significant portion of the hydrogen produced is consumed by further oxidation, as also reported by Christensen et al. [31] for non-catalytic partial oxidation of ethanol. The CO, CO_2 and CH_4 are most likely produced by reforming reactions and C_2H_4 is formed by dehydration of ethanol.

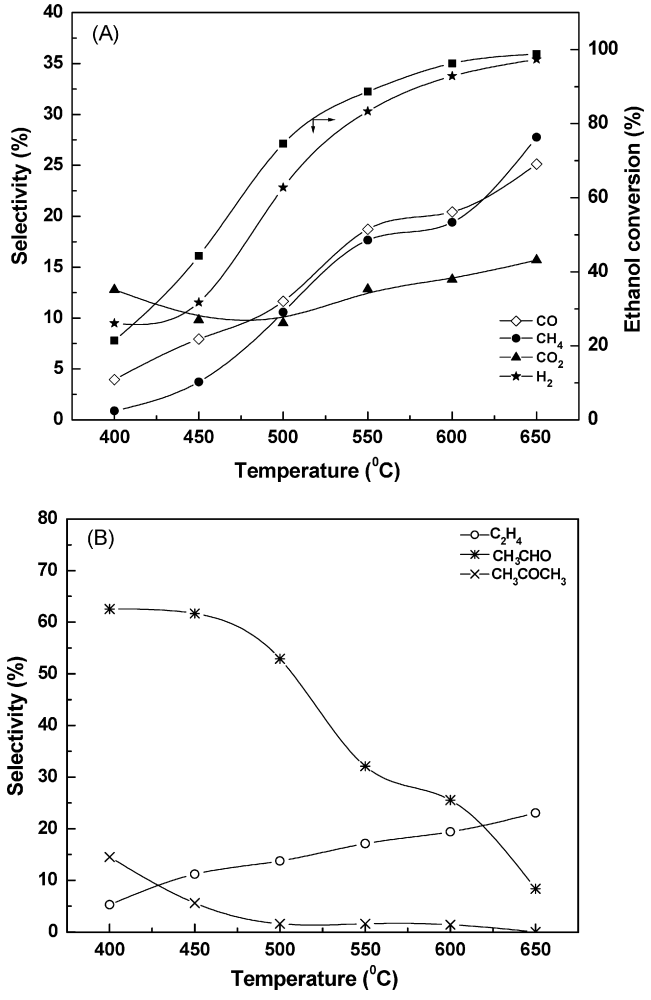

Fig. 1. Variation in conversion of ethanol and product selectivities with temperature for non-catalytic oxidative steam reforming. (A) Conversion and product selectivities of CO, CH_4, CO_2 and H_2. (B) Product selectivities of C_2H_4, CH_3CHO and CH_3COCH_3.

3.2. Catalytic steam reforming

The effect of temperature on ethanol conversion and product selectivities in the absence of oxygen is shown in Fig. 2. Conversion increased with temperature and was greater than 90% at 500 °C. In the steam reforming process, the main products were H_2, CO, CH_4 and CO_2 but at lower temperature (<450 °C) small amounts of CH_3CHO was also obtained. Above 450 °C, the CH_3CHO selectivity became zero. Selectivity to H_2 and CO_2 increased with temperature, selectivity to CH_4 decreased with temperature whereas the CO selectivity passed through a minima at 500 °C. The results show that, 30 wt.%Ni/$Ce_{0.74}Zr_{0.26}O_2$ catalyst is active for steam reforming of ethanol. In such catalysts, both nickel and ceria can affect the activity and product selectivities. The effect of CeO_2 content of Ni/CeO_2-ZrO_2 catalysts has been reported earlier [28]. The reducibility and the thermal stability of CeO_2 are greatly enhanced by the addition of ZrO_2 due to the formation of solid solution [32]. The smaller size of Zr cation modifies the cubic fluorite structure of CeO_2, resulting in enhanced oxygen mobility and oxygen storage capability [33]. Due to this enhanced oxygen mobility, CeO_2 in CeO_2-ZrO_2 solid solution can undergo rapid oxidation–reduction cycles and the capability of redox couple Ce^{4+}–Ce^{3+} is enhanced. Consequently, the activity of CeO_2 for oxidation reaction increases significantly by the addition of ZrO_2 [26]. Laosiripojana and Assabumrungrat [34] have discussed the role of CeO_2 on promoting the ethanol steam reforming activity. During reaction,

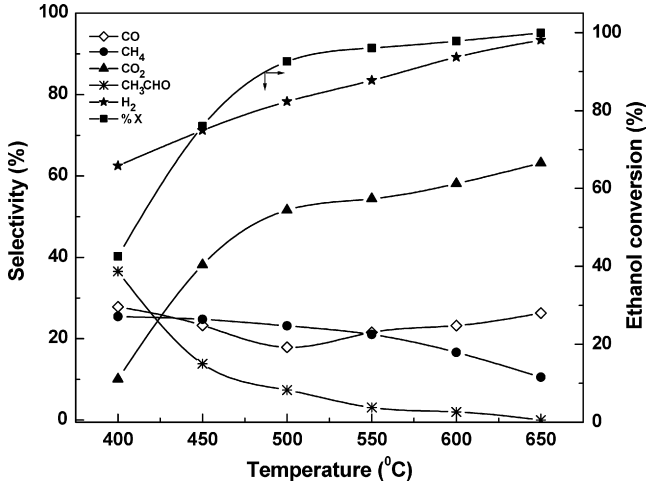

Fig. 2. Variation in conversion of ethanol and product selectivities of ethanol steam reforming reaction with temperature.

the hydrocarbons such as ethanol, ethylene, ethane and methane are adsorbed on the ceria site or lattice oxygen. The reaction is controlled by surface oxygen. Subsequently, the lattice oxygen is regenerated by oxygen containing compounds such as steam present in the system. CeO_2 can also suppress CH_4 formation by providing active oxygen species which are formed by the partial oxidation of Ce sites under reforming conditions [35]. Moreover, CeO_2 is also active for catalyzing the water gas shift reaction [16]. Therefore, the high activity of 30 wt.%Ni/$Ce_{0.74}Zr_{0.26}O_2$ catalyst may be due to the high oxygen storage capacity of the catalyst and the higher water gas shift activity of CeO_2.

Haryanto et al. [18] have summarized the reaction pathways that can occur during SR over metal catalysts. The product distribution suggests that the important reaction occurring over 30 wt.%Ni/$Ce_{0.74}Zr_{0.26}O_2$ catalyst are:

$$C_2H_5OH \rightarrow CH_3CHO + H_2 \quad (1)$$

$$C_2H_5OH \rightarrow C_2H_4 + H_2O \quad (2)$$

$$CH_3CHO = CO + CH_4 \quad (3)$$

$$CH_3CHO + H_2O \rightarrow 2CO + 3H_2 \quad (4)$$

$$CH_4 + H_2O \rightleftharpoons CO + 3H_2 \quad (5)$$

$$CO + H_2O \rightleftharpoons CO_2 + H_2 \quad (6)$$

During steam reforming, acetaldehyde is mainly formed due to dehydrogenation of ethanol according to reaction (1). The decrease in selectivity to CH_4 and increase in the selectivity to CO_2 and H_2 with temperature suggest that SR of methane and the water gas shift (WGS) have not reached equilibrium. On this catalyst, above 550 °C, rates of decomposition and reforming of CH_3CHO are much faster than rate of formation of CH_3CHO, resulting in very low selectivity to CH_3CHO at higher temperature. It can be observed that at lower temperatures selectivity to CO and CH_4 are equal, suggesting that CO and CH_4 formation takes place by dissociation of CH_3CHO (reaction (3)). At higher temperature, the product composition is controlled by methane reforming reaction and WGS reaction [14]. When temperature increases, methane and water are consumed resulting in increase in the selectivities to H_2 and CO_2.

Without oxygen, a significant amount of side products (CO and CH_4) were obtained which need to be reduced. Therefore, the effect of oxygen addition on selectivity of products and conversion was examined.

3.3. Catalytic oxidative steam reforming

Oxidative steam reforming was investigated at different flow rates and temperature. The effect of flow rate of ethanol–water mixture on conversion and product selectivities was studied at 600 °C. For these experiments, the ethanol flow was varied from 0.02 to 0.40 ml/min; this corresponds to variation in W/F_{A0} from 1.6 to 4.1 gcat h mol^{-1}, where W is the mass of catalyst and F_{A0} is the inlet molar flow rate of ethanol. For this set of runs, molar ratio of O_2/EtOH was kept fixed at 0.5. Variation in ethanol conversion and product selectivities with W/F_{A0} is shown in Fig. 3. At all flow rates, ethanol conversion was

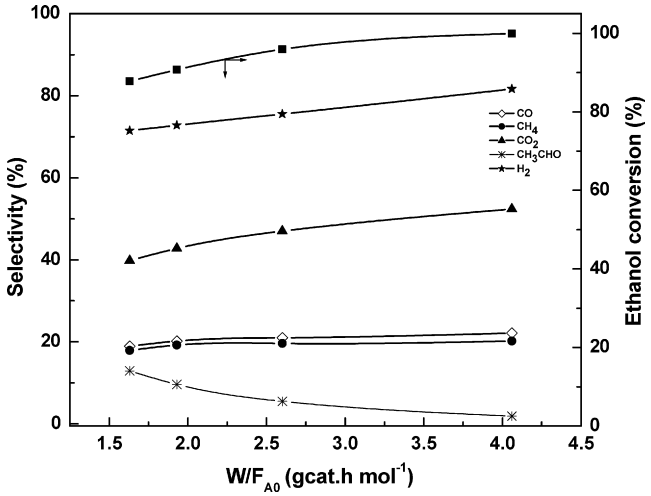

Fig. 3. Variation in conversion of ethanol and product selectivities with W/F_{A0} during oxidative steam reforming (Temperature = 600 °C; O_2/EtOH = 0.5 mol/mol).

greater than 88% and oxygen conversion was complete. The main products were H_2, CO, CH_4 and CO_2 but at lower W/F_{A0} small amount of CH_3CHO was also observed. With increasing W/F_{A0}, selectivity to H_2 and CO_2 increased. The selectivities to CO and CH_4 were not significantly affected by changing the flow rate.

The effect of oxygen addition for a constant H_2O/EtOH molar ratio on conversion and product selectivity is shown in Fig. 4. For these runs O_2/EtOH molar ratio was varied from 0.5 to 1.5 and nitrogen flow rate changed accordingly to keep the total flow constant. For this set of runs, W/F_{A0} was kept fixed at 4.1 gcat h mol^{-1}. As shown in Fig. 4A, conversion increased with increasing O_2/EtOH; the effect was more significant at lower temperatures (<450 °C). At lower temperature (<500 °C), in absence of oxygen the conversion was less than 80%. When a small amount of oxygen (O_2/EtOH = 0.5 mol/mol) was added, the conversion of ethanol became 92% at 400 °C. Complete conversion of ethanol was observed even at 400 °C at an O_2/EtOH molar ratio of 1.0. In presence of oxygen, over the whole tested range of O_2/EtOH molar ratio, the ethanol and oxygen conversion were almost complete at a temperature higher than 400 °C.

The variation in product selectivities with O_2/EtOH molar ratio at different temperatures is shown in Fig. 4. Below 550 °C, the H_2 selectivity showed a maxima, whereas at higher temperatures, selectivity to H_2 decreased with increasing O_2/EtOH molar ratio. At a constant O_2/EtOH, selectivity to hydrogen increased with temperature (Fig. 4B). Selectivity to CO passed through a minima with increasing oxygen content (Fig. 4C). The lowest selectivity to CO (13.7%) was obtained at 500 °C at an O_2/EtOH molar ratio of 0.5. In the temperature range of 400–550 °C, selectivity to CH_4 decreased with an increase in O_2/EtOH. At higher temperature, selectivity to CH_4 increased with oxygen content up to a O_2/EtOH molar ratio of 1.0 and then became almost constant. The selectivity to CO_2 at 400 °C increased with an increase in O_2/EtOH ratio but at higher temperatures, the CO_2 selectivity passed through a maxima on increasing the O_2 content of feed. Selectivity to CH_3CHO

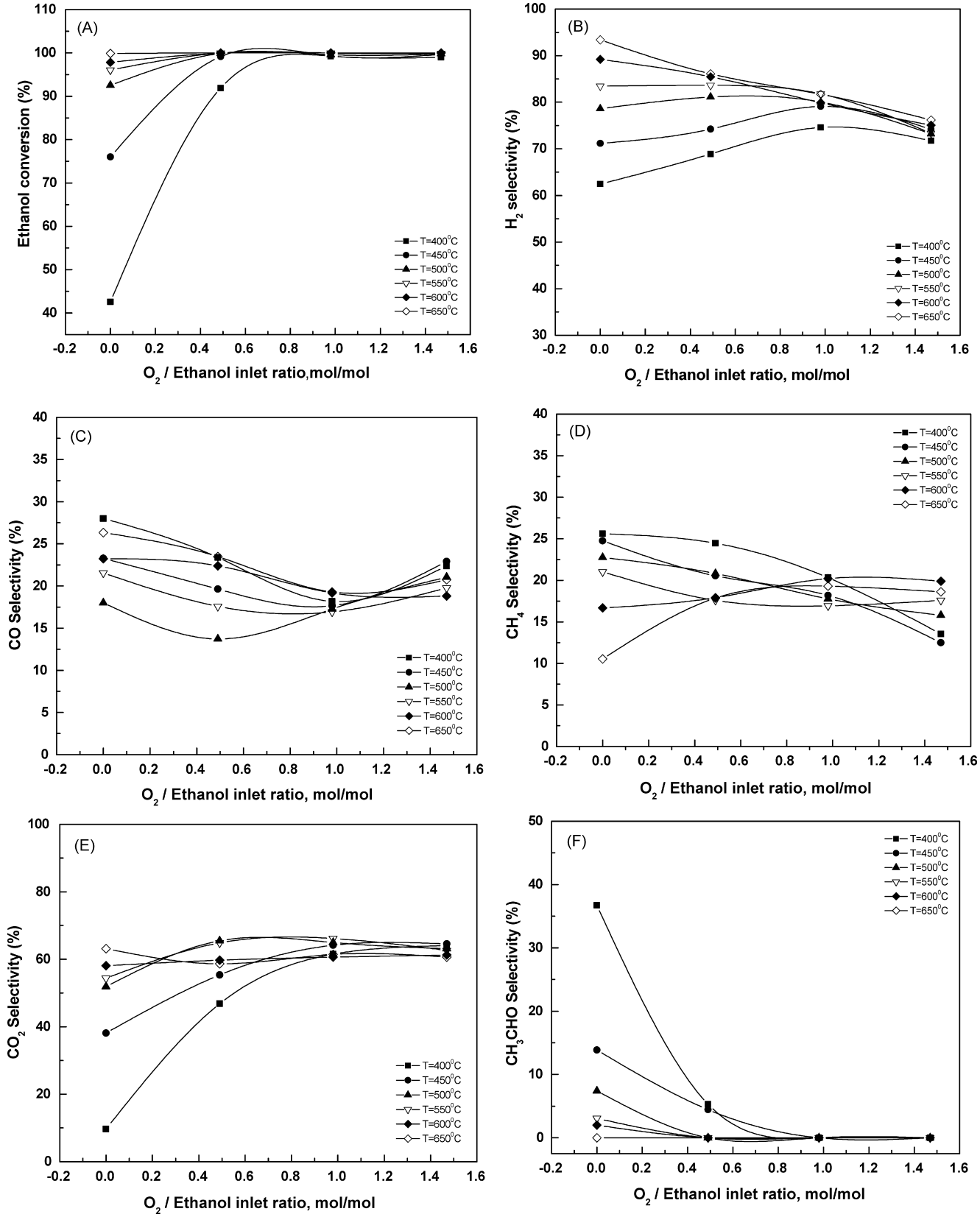

Fig. 4. Variation in ethanol conversion and product selectivities with inlet O_2/EtOH molar ratio at different temperatures for oxidative steam reforming (A) conversion; (B) H_2 selectivity (C) CO selectivity; (D) CH_4 selectivity (E) CO_2 selectivity; (F) CH_3CHO selectivity.

decreased with increasing oxygen content as well as temperature (Fig. 4F).

In the presence of oxygen, the following reactions can also occur [36]:

$$H_2 + \tfrac{1}{2}O_2 = H_2O \quad (7)$$

$$CO_2 + \tfrac{1}{2}O_2 = CO_2 \quad (8)$$

$$CH_4 + 2O_2 = CO_2 + 2H_2O \quad (9)$$

$$C_2H_5OH + \tfrac{1}{2}O_2 = CH_3CHO + H_2O \quad (10)$$

$$C_2H_5OH + 3O_2 = 2CO_2 + 3H_2O \quad (11)$$

The observed selectivity trends during OSR can be explained based on the proposed reaction scheme. The increase in the selectivities to H_2 and CO_2 with increasing W/F_{A0} (Fig. 3) indicates that water gas shift reaction and the methane steam reforming (MSR) reactions have not reached equilibrium. To verify this, the change in the mass action ratios of methane steam reforming ($MAR_{SR} = p_{H_2}^3 p_{CO}/p_{CH_4} p_{H_2O}$) and water gas shift reaction ($MAR_{WGS} = p_{CO_2} p_{H_2}/p_{CO} p_{H_2O}$) with W/F_{A0} was calculated from the experimental data and this variation is shown in Fig. 5. As can be seen from Fig. 5, the WGS reaction nearly approaches equilibrium at the highest W/F_{A0} whereas the MSR reaction is still far from equilibrium.

In the presence of oxygen, reactions (7)–(11) are favored. At low oxygen concentration (O_2/EtOH = 0.5 mol/mol), the CO consuming reactions are faster than the CO formation reactions. At higher O_2/EtOH ratios, the CO oxidation reaction is favored resulting in larger amounts of CO_2. As a result, according to mass action, the reverse WGS is favored, thereby increasing the selectivity to CO. Due to the higher rate of ethanol combustion (reaction (11)) as compared to ethanol dehydrogenation, the selectivity to CH_3CHO significantly decreases in the presence of oxygen.

The methane combustion results in a decrease in the selectivity to CH_4 in the presence of O_2. Unexpectedly, at temperature above 600 °C, the selectivity to CH_4 increased in the presence of small amounts of O_2. In there study of auto-thermal reforming of ethanol on rhodium catalyst, Vesselli et al. [37] also reported higher methane concentration in the outlet stream in the presence of oxygen. They postulated that presence of O_2 favors CH_3 recombination with adsorbed hydrogen to CH_4, probably due to a site blocking mechanism. Another reason for the higher selectivity to CH_4 could be the enhanced rate of the reverse methane steam reforming reaction, due to the higher concentration of CO. The increase in selectivity to H_2 with addition of small amount of oxygen at lower temperatures is attributed to the significant decrease in the selectivity to CH_3CHO. At higher temperatures, the hydrogen selectivity decreased due to hydrogen oxidation reaction. Klouz et al. [36] in their study of OSR of ethanol over Ni/Cu catalyst also reported a similar trend for selectivity to H_2 with increasing O_2/EtOH molar ratio. By comparing the results obtained with and without oxygen, we observe that, by the addition of oxygen, activity of the catalyst increased significantly and the product selectivities were also affected. Since the main product of interest is hydrogen, the effect of inlet molar ratio of O_2/EtOH on hydrogen yields was calculated and is shown in Table 1. As can be seen from this table, at temperatures ≤500 °C, hydrogen yields are highest at a O_2/EtOH molar ratio of 0.5; whereas at higher temperatures, higher yields are obtained in the absence of oxygen. The other advantage of using small amounts of oxygen in the feed is on the energy requirements. To check the endothermicity or exothermicity of the ethanol reforming reaction, the overall heat of reaction at 650 °C was estimated for both SR and OSR. For each case, the measured product distribution

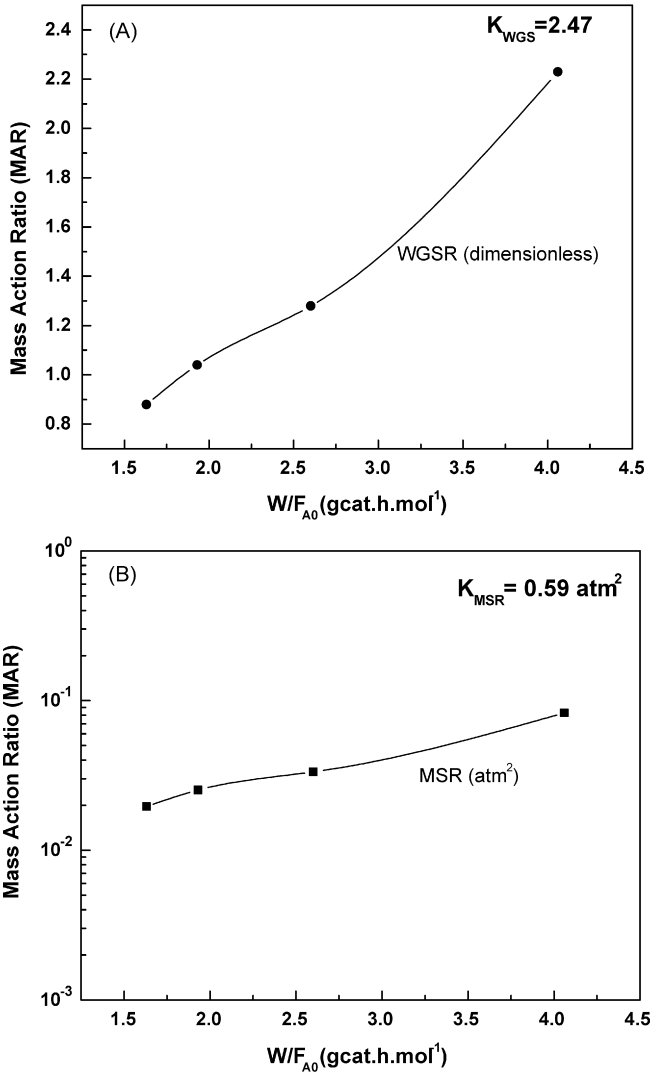

Fig. 5. Variation in mass action ratios with W/F_{A0} for water-gas shift reaction (A) and methane reforming reaction (B).

Table 1
Variation in hydrogen yield with temperature and O_2/EtOH molar ratio

O_2/EtOH ratio (mol/mol)	H_2 yield (mol of H_2/mol of EtOH fed)					
	400 °C	450 °C	500 °C	550 °C	600 °C	650 °C
0	1.29	2.40	3.41	4.26	5.67	5.64
0.5	2.08	2.92	3.52	3.57	4.23	4.34
1.0	2.21	2.55	2.80	2.97	3.18	3.40
1.5	1.31	1.38	1.63	1.76	2.23	2.24

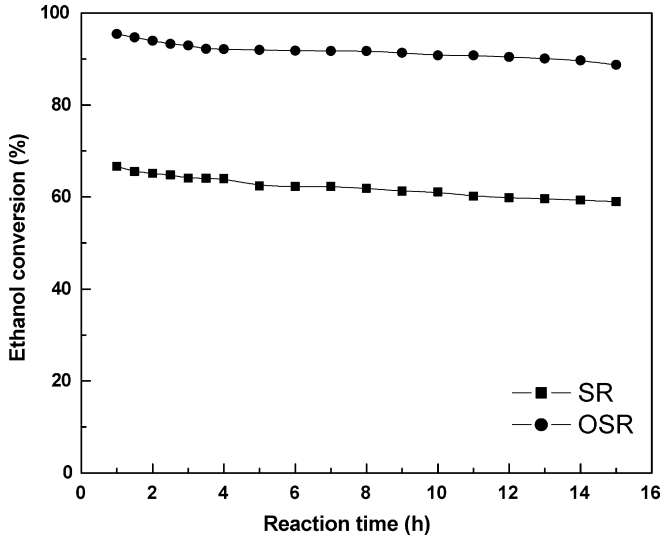

Fig. 6. Variation in ethanol conversion with run time over 30 wt.%Ni/$Ce_{0.74}Zr_{0.26}O_2$ catalyst $T = 600\,^{\circ}C$; $W/F_{A0} = 0.80$ gcat h mol^{-1}; O_2/EtOH = 0.5 (for OSR).

was utilized to represent the overall reforming reaction. The standard heats of formation of reactants and products were obtained from Reid et al. [38]. The calculated value for the overall heat of reaction for SR was 164.6 kJ/mol whereas at an O_2/EtOH of 0.5, the overall heat of reaction was −86.5 kJ/mol. Thus, small amounts of oxygen can be beneficial.

3.4. Catalytic stability and coke formation

Stability is an important characteristic of any catalyst that determines its efficient use in a reaction. As discussed in the previous section, at the space time used for the catalytic activity and product distribution studies, the conversion for both SR and OSR was 100%. In order to highlight the difference in activity and deactivation rate of the catalyst in SR and OSR, the catalyst stability comparison was carried out at 600 °C with a lower space time ($W/F_{A0} = 0.80$ gcat h mol^{-1}). The variation in ethanol conversion with run time is shown in Fig. 6. For the OSR run, the O_2/EtOH mol ratio was 0.5. As can be seen from this figure, oxygen significantly improved the activity. For both SR and OSR, till a run time of 4 h, the catalyst deactivation rate was faster, and beyond that the rate of deactivation decreased. Between a run time of 4–15 h, for SR, the ethanol conversion decreased by 4.9% whereas for OSR the decrease was 3.4%. Therefore, all the experimental data reported were taken after 4 h of reaction as stated earlier. The result shows that, the Ni/CeO_2-ZrO_2 is active for ethanol reforming for long time and oxygen positively affects the catalyst stability. Similar kind of activity trend

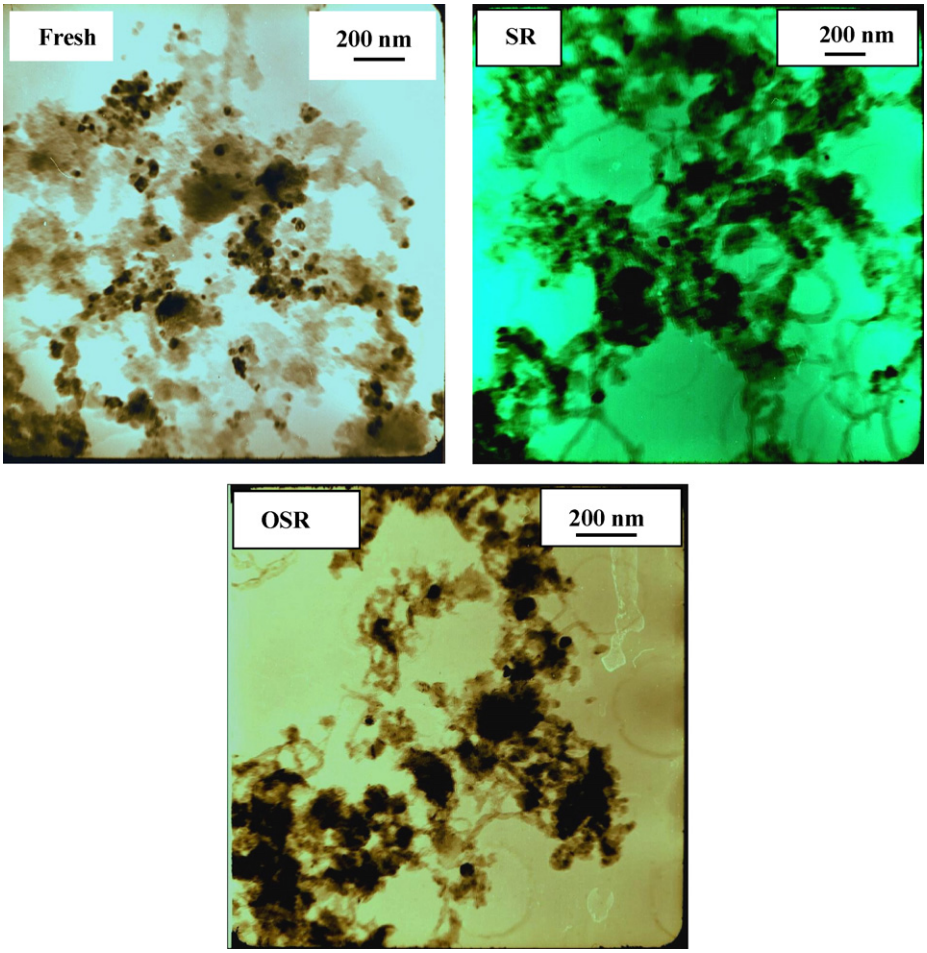

Fig. 7. TEM images of fresh and used 30 wt.%Ni/$Ce_{0.74}Zr_{0.26}O_2$ catalyst.

was reported by Cavallaro et al. [13] for SR of ethanol over Rh/Al_2O_3 catalyst. Srinivas et al. [39] reported that 40 wt.% Ni/CeO_2 (30 wt.%)-ZrO_2 (30 wt.%) was active for more than 500 h without deactivation in SR of ethanol.

The amount of carbon deposited on the catalyst after 15 h of run time was measured by CHNS elemental analysis. A considerable amount of carbon was formed for both SR (6.03 mmolC $gcat^{-1}$ h^{-1}) and OSR (3.3 mmolC $gcat^{-1}$ h^{-1}). Laosiripojana and Assabumrungrat [34] proposed possible pathways of coke formation during SR of ethanol. According to them, at low temperature, the coke formation takes place mainly due to the hydrogenation of CO and CO_2 to form water and carbon. At higher temperature, the coke formation occurs mainly due to decomposition of methane, ethane, ethylene and the Boudouard reaction. Similarly, Liguras et al. [14] reported that ethane and ethylene are the strong promoters of carbon formation. On CeO_2 surface, the carbonaceous compounds (CO, CH_4, C_2H_4, C_2H_6) can combine with the lattice oxygen resulting in reduced coke deposition. In a related study on partial oxidation of CH_4, it has been reported that carbon formation is lower on Ni/CeO_2-ZrO_2 catalyst as compared to Ni supported on CeO_2 or ZrO_2 catalysts [40]. In contrast to these studies, Frusteri et al. [24] reported that, in the absence of oxygen, CeO_2 promotes coke formation by hydrocarbon decomposition due to strong interaction with the adsorbed reaction intermediate species like acetaldehyde or ethoxy involved in the reaction mechanism. They reported approximately 2 and 0.3 mmolC $gcat^{-1}$ h^{-1} for steam and auto-thermal reforming of ethanol over Ni/CeO_2 catalyst, respectively. In this study, the carbon formation is little higher; this is may be due to the low nickel area of the catalyst or a low metal support interaction [41,42]. The coke formation was reduced significantly (≈45%) in the presence of small amount (O_2/EtOH = 0.5 mol/mol) of oxygen.

For the reforming of hydrocarbon and oxygenated compound over Ni/CeO_2 and Ni/CeO_2-ZrO_2 catalysts, two types of coke formation have been reported depending on the mechanism of coke formation. Frusteri et al. [24] observed both filamentous and agglomerated carbon in SR over Ni/CeO_2 catalyst whereas in OSR only agglomerated carbon was detected. The TEM images of the fresh and used catalysts are shown in Fig. 7. The nickel crystallite for the fresh catalysts was in the range of 15–20 nm which is in agreement with the value calculated using XRD. For the used catalyst, filamentous and agglomerated carbon were detected for both SR and OSR (Fig. 7). Comparing the TEM of fresh and used catalysts, it was observed that there was no significant difference in the nickel particle size indicating that catalyst sintering was not significant.

4. Conclusions

30 wt.%$Ni/Ce_{0.74}Zr_{0.26}O_2$ catalyst is active and selective for hydrogen production by steam reforming. For SR at a temperature of 650 °C, ethanol conversion of 100% can be achieved with a maximum hydrogen selectivity of 93.4%. Even in the absence of a catalyst, ethanol conversion during oxidative reforming of ethanol is appreciable above 500 °C; however the selectivity to hydrogen is low. In the presence of small amount of oxygen (O_2/EtOH = 0.5 mol/mol), the catalyst activity is enhanced significantly, and at temperatures less than 500 °C, the hydrogen yields are also higher than without oxygen. Increasing the O_2/EtOH molar ratio beyond 0.5 has no added advantage, as the hydrogen yields are lower. At temperatures above 500 °C, hydrogen yields are higher in the SR process. Measurable amounts of coke are formed in both SR and OSR but do not affect catalyst activity significantly till a run time of 15 h.

References

[1] Ayhan Demirbas, Prog. Energy Comb. Sci. 33 (2007) 1.
[2] M.F. Demirbas, Mustafa Balat, Energy Conv. Manage. 47 (2006) 2371.
[3] A.N. Fatsikostas, D.I. Kondarides, X.E. Verykios, Catal. Today 75 (2002) 145.
[4] P. Ramirez de la Piscina, N. Homs, in: S. Minteer (Ed.), Ethanol Reformation to Hydrogen in "Alcohol Fuels", Taylor & Francis, CRC, 2006, p. 233.
[5] X.E. Verykios, Int. J. Hydrogen Energy 28 (2003) 1045.
[6] A. Heinzel, B. Vogel, P. Hubner, J. Power Sources 105 (2002) 202.
[7] Y.H. Chin, R. Dagle, J. Hu, A.C. Dohnalkova, Y. Wang, Catal. Today 77 (2002) 79.
[8] B. Lindstrom, L.J. Petterson, Int. J. Hydrogen Energy 26 (2001) 923.
[9] T. Takasashi, M. Inoue, T. Kai, Appl. Catal. A: Gen. 218 (2001) 189.
[10] F. Marino, M. Boveri, G. Baronetti, M. Laborde, Int. J. Hydrogen Energy 29 (2004) 67.
[11] G.A. Deluga, J.R. Salge, L.D. Schmidt, X.E. Verykios, Science 303 (2004) 993.
[12] S. Fernando, M. Hanna, Energy Fuels 18 (2004) 1695.
[13] S. Cavallaro, V. Chiodo, S. Freni, N. Mondello, F. Frusteri, Appl. Catal. A: Gen. 249 (2003) 119.
[14] D.K. Liguras, D.I. Kondarides, X.E. Verykios, Appl. Catal. B: Environ. 43 (2003) 345.
[15] J. Llorca, J.A. Dalmon, P.R. Piscina, N. Homs, Appl. Catal. A: Gen. 243 (2003) 261.
[16] F. Aupretre, C. Descorme, D. Duprez, Catal. Commun. 3 (2002) 263.
[17] J. Sun, X.P. Qiu, F. Wu, W.T. Zhu, Int. J. Hydrogen Energy 30 (2005) 437.
[18] A. Haryanto, S. Fernando, N. Murali, S. Adhikari, Energy Fuels 19 (2005) 2098.
[19] P.D. Vaidya, A.E. Rodrigues, Chem. Eng. J. 117 (2006) 39.
[20] V. Fierro, O. Akdim, H. Provendier, C. Mirodatos, J. Power Sources 145 (2005) 659.
[21] S. Freni, S. Cavallaro, N. Mondello, L. Spadaro, F. Frusteri, Catal. Commun. 4 (2003) 259.
[22] S. Cavellaro, V. Chiodo, A. Vita, S. Freni, J. Power Sources 123 (2003) 10.
[23] S. Velu, K. Suzuki, M. Vijayaraj, S. Barman, C.S. Gopinath, Appl. Catal. B: Environ. 55 (2005) 287.
[24] F. Frusteri, S. Freni, V. Chiodo, S. Donato, G. Bonura, S. Cavallaro, Int. J. Hydrogen Energy 31 (2006) 2193.
[25] J. Kaspar, P. Fornasiero, M. Graziani, Catal. Today 50 (1999) 285.
[26] H.S. Roh, H.S. Potdar, K.W. Jun, Catal. Today 93–95 (2004) 39.
[27] S. Pengpanich, V. Meeyoo, T. Rirksomboon, Catal. Today 93–95 (2004) 95.
[28] P. Biswas, D. Kunzru, Int. J. Hydrogen Energy 32 (2007) 969–980.
[29] N. Laosiripojana, S. Assabumrungrat, Appl. Catal. A: Gen. 290 (2005) 200.
[30] A.M. Arias, M.F. Garcia, V. Ballesteros, L.N. Salamanca, J.C. Conesa, C. Otero, J. Soria, Langmuir 15 (1999) 4796.
[31] D.O. Christensen, P.L. Silvestone, E. Croiset, R.R. Hudgins, Ind. Eng. Chem. Res. 43 (2004) 2636.
[32] R.D. Monte, J. Kaspar, Catal. Today 100 (2005) 27.
[33] A. Trovarelli, F. Zamar, J. Llorca, C. Leitenburg, G. Dolcetti, J.T. Kiss, J. Catal. 169 (1997) 490.

[34] N. Laosiripojana, S. Assabumrungrat, Appl. Catal. B: Environ. 66 (2006) 29.
[35] H.S. Roh, Y. Wang, D.L. King, A.P. Platon, Y.H. Chin, Catal. Lett. 1–2 (2006) 15.
[36] V. Klouz, V. Fierro, P. Denton, H. Katz, J.P. Lisse, S. Bouvot-Mauduit, C. Mirodatos, J. Power Sources 105 (2002) 26.
[37] E. Vesselli, G. Comelli, R. Rosei, S. Freni, F. Frusteri, S. Cavallaro, Appl. Catal. A: Gen. 281 (2005) 139.
[38] R.C. Reid, J.M. Prausnitz, B.E. Poling, The properties of Gases & Liquids, McGraw-Hill Int. Ed., 1988.
[39] D. Srinivas, C.V.V. Satyanarayana, H.S. Potdar, P. Ratnasamy, Appl. Catal. A: Gen. 246 (2) (2003) 323.
[40] S. Xu, X. Wang, Fuel 84 (2005) 563.
[41] N. Nichio, M. Casella, O. Ferretti, M. Gonzalez, C. Nicot, B. Moraweck, R. Frety, Catal. Lett. 42 (1996) 65.
[42] Y.H. Hu, E. Ruckenstein, Catal. Lett. 36 (1996) 145.